**Proceedings of IMECE'04**
**2004 ASME International Mechanical Engineering Congress & Exposition**
**Anaheim, California, November 13-19, 2004**

# IMECE2004-61788

## Tumor Imaging Through Temporal Log-Slope Difference Mapping of Transient Radiation Signals

Zhixiong Guo*
Department of Mechanical and Aerospace Engineering
Rutgers, The State University of New Jersey
98 Brett Road, Piscataway, NJ 08854

Siew Kan Wan
Department of Mechanical and Aerospace Engineering
Rutgers, The State University of New Jersey
98 Brett Road, Piscataway, NJ 08854

David A. August
UMDNJ/Robert Wood Johnson Medical School and The Cancer Institute of New Jersey
New Brunswick, NJ 08903

Stanley M. Dunn
Department of Biomedical Engineering
Rutgers University
Piscataway, NJ 08854

John L. Semmlow
Department of Biomedical Engineering
Rutgers University
Piscataway, NJ 08854

### ABSTRACT

A novel optical approach is proposed for cancerous tumor detection using transient radiation signals. In this method, target tissue is illuminated by near-infrared ultrashort laser pulses from various surface source points, and backscattered time-resolved light signals are collected at the same surface points. By analyzing the log-slopes of decaying signals over all points on the source-detection grid, a log-slope distribution on the surface is obtained. After administration of absorption contrast agents, the presence of cancerous tumors increases the decaying steepness of the transient signals. The mapping of log-slope difference between native tissue and absorption-enhanced cancerous tissue indicates the location and projection of tumors on the detection surface. In this paper, we examine this method through the detection of a small tumor in a model tissue phantom via computer simulation. The model has a spherical tumor of 6 mm in diameter embedded at the tissue center. Monte Carlo methods were employed to simulate the light transport and signal measurement. It is shown that the tumor in the tissue model can be accurately projected onto the detection surface by the proposed log-slope difference mapping method. The image processing is very fast and does not require any inverse optimization in image reconstruction.

Keywords: Transient radiation transfer, optical imaging, cancer detection, temporal log-slope, absorption contrast agent, ultrafast laser, Monte Carlo simulation.

*Corresponding author, e-mail: guo@jove.rutgers.edu

### INTRODUCTION

Early diagnosis of tumors is thought to represent an important opportunity to reduce both the morbidity and mortality among cancer patients. Chest x-rays, computed tomography, and mammograms are the most commonly used modalities, but these methods can be costly and induce radiation exposure. Therefore, a great need exists for new noninvasive methods that pose less safety concerns, are low cost, portable and can be made widely available to large segments of the population.

Optical imaging methods are excellent candidates to provide an alternative imaging modality. Near-infrared (NIR) optical imaging has become increasingly attractive in recent years because NIR radiation is non-ionizing and the approach can lead to devices that are very compact and cost-effective. Furthermore, optical imaging can provide not only structural information [1-7] and functional information [8-11], but also cellular and molecular information [12,13].

Wavelengths in the NIR range, especially between 700-900nm are widely used in research for diffuse optical tomography (DOT) because this spectral window has the lowest overall tissue absorption. In other words, light in that range has a much greater penetration depth allowing deep imaging up to 10 centimeters. This is sufficient for many potential clinical applications, such as breast cancer screening and diagnosis. In DOT techniques, the target tissue is illuminated by a NIR laser. Measurements of light signals around the tissue boundary are made and used to reconstruct tissue images of optical parameters. Diseases are detected

and/or diagnosed based on the difference of optical properties between normal and diseased tissues.

The most challenging task in utilizing DOT is the fact that NIR light is highly scattered in human tissues. For highly diffused NIR light in biologic tissues, the temporal and/or spatial intensity response sensed by a detector is not only determined by the optical properties along a direct path between the source and detector, but also by the optical properties in large surrounding regions as described in random walk theory. Therefore, the image reconstruction in diffuse optical tomography is a formidable inverse problem. Previously, most forward modeling approaches use a simplified diffusion approximation [3-7]. Rigorous radiation transfer simulation [15-17] is more appropriate, however, because biological tissues are generally heterogeneous and may contain low-scattering and/or high-absorbing regions. Given the complexity of both the distribution of tissue optical properties and a forward model approach, an image reconstruction in a typical DOT may take several hours to several days even with the latest computation technology.

A much faster method to detect tumors can be based on the relative absorption contrast between the cancerous tumors and surrounding normal tissues, rather than the solution of the distributions of tissue optical parameters. Some recent reports have shown that the NIR absorption in cancerous regions can be greatly enhanced by the addition of absorbing dyes that have close affinity to the tumor [3,12]. The strong absorption will have a greater attenuation effect on the light signals detected at the tissue surface, especially for detectors most closely located to the cancerous tumor. This will result in an increase of decaying steepness in the temporal light signals. By measuring the temporal slopes of the logarithmically decaying signals over all detection points, a log-slope distribution on the tissue surface is obtained. The area with large log-slope values may represent a projection of tumors. In this approach, the complicated inverse image reconstruction is avoided.

The feasibility of the temporal log-slope approach in detecting a highly absorbing inhomogeneity in turbid media has been recently demonstrated [18] both experimentally and through simulation using a tiny graphite inclusion inside a homogeneous tissue phantom. It was motivated by several published studies [19-26] that investigated the laser pulse response of both transmitted and backscattered signals in turbid media. The research on time-resolved reflectance measurement can be retraced to the pioneering work of Chance et al. [1988] and Patterson et al. [1989], in which the optical properties of tissues were obtained from fitting the experimental data with a standard solution of the diffusion theory for a semi-infinite homogeneous medium. They used information like the measured time of maximum signal and the long-time, asymptotic log slope (ALS) of the reflected pulse. Brewster and Yamada [20] conducted a computational and experimental investigation regarding the feasibility of determining of optical properties of turbid media from picosecond time-resolved light scattering measurements in conjunction with diffusion theory predictions and Monte Carlo simulations. They also used the concept of the long-time asymptotic log slope of the time-resolved signals. Recent studies by Guo and co-authors [16, 17] extended these transient laser pulse investigations to two- and three-dimensional non-homogeneous tissue phantoms. They observed variations in the temporal log-slope of the detected signals at an intermediate time stage in the presence of a relatively high absorbing tumor in the tissue phantoms.

Guo's log-slope approach is different from the prior ALS studies of others in three aspects: (1) Guo analyzed the temporal log slopes in a partition of the temporal signal curves at an intermediate time range where the signals may have incorporated the inhomogeneity information; while others considered the only ALS at the long time stage where the signals are usually very weak and the uncertainty of measurement is high. (2) Guo's approach does not involve any forward and inverse modeling and thus, does not directly provide the optical properties of the medium; while others tried to measure the optical properties in conjunction with modeling efforts. (3) Guo's approach is used for finding inhomogeneities in multi-dimensional geometries; while other approaches are used in a homogeneous medium of semi-infinite thickness.

In our previous temporal log-slope approach, however, there is a fuzzy boundary around the absorbing inhomogeneity area and the edge effect [18] (signals decay fast in detectors located near surface edge) on the detecting surface is very pronounced. Here we propose a modified version of the log-slope approach, i.e., mapping of temporal log-slope difference on the detection surface between log-slope distributions before and after administration of absorption contrast agent. Such a subtraction operation will eliminate the edge effect and diminish the fuzzy boundary of images. The feasibility of the proposed temporal log-slope difference mapping approach for cancer detection is studied by simulating light propagation in tissue phantom implanted with spherical tumors and evaluating the light detection from a coincident laser source over a predefined grid on the tissue surface. The propagation of photon in the tissue phantom is simulated via our 3-D transient Monte Carlo radiative transfer method [22, 23].

## MODEL AND IMAGING

As a proof study, the detection model consists of a homogeneous cuboidal tissue phantom embedded with a spherical tumor located at the center (see Fig. 1). The tissue phantom's dimensions are 20 x 20 x 20 $mm^3$, and the spherical tumor has a diameter of 6mm. The NIR optical properties of the tissue phantom have been assigned to mimic biologic tissue. We assume the reduced scattering and absorption coefficients of the tissue are 1.0 $mm^{-1}$ and 0.005 $mm^{-1}$, respectively. These typical values are selected in line with the studies in the literature [1-9]. Optical properties of living tissue vary with light wavelength and physiological functions. The measured optical properties for different individuals are also different. All these will tremendously complicate the clinical use of conventional DOT techniques. However, they do not practically influence the present imaging method because the present method is based on the detection of relative absorption change. The exact value of tissue optical properties and their variations in actual tissues are insignificant. Hence, we may assume a homogeneous profile for tissue optical properties when contrast agents are used. The difficulty in the treatment of the heterogeneity of tissue structure and properties is overcome in this imaging method.

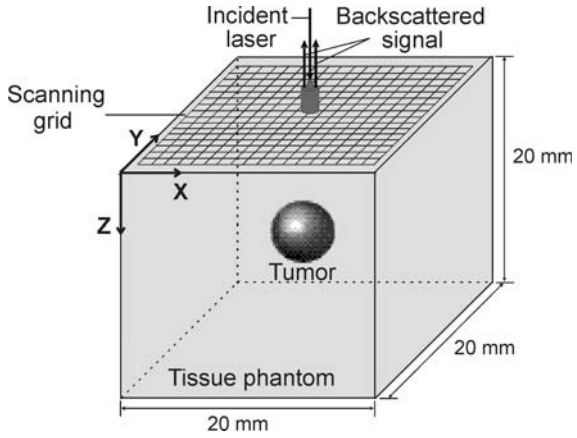


Figure 1 – Detection model: a spherical tumor of 6mm in diameter embedded at the center of a 20 x 20 x 20 $mm^3$ tissue phantom

After injection of absorbing dyes, the absorption coefficient in the cancerous tumor region is assumed to be 0.2$mm^{-1}$, while it is 0.01 $mm^{-1}$ in the healthy tissue region. This corresponds to an absorbing dye uptake ratio of 40:1. The absorption contrast between the absorption-enhanced tumor and the healthy tissue is therefore 20:1. The absorption coefficient of malignant cancerous tissue is greater than that of healthy tissue, because increased blood flow leads to higher concentration or accumulation of oxy- and deoxy-hemoglobin (two natural absorbing chromophores inside human body at NIR wavelengths). As compared with the significant absorption augmentation through absorbing dye administration, however, this natural absorption contrast between cancerous and healthy tissues is negligible. The refractive index of tissue phantom is assumed to be 1.4.

The laser delivery and detection system is set up so that the incident laser and backscattered signal coincide with each other. Ultrafast laser pulses are set to be delivered across a circular area with an effective radius of 0.1mm. The intensity distribution is assumed to be a Gaussian profile with its peak intensity located at the center of the circular area. The scanning grid for detection model consists of a 19 x 19 equally spaced mesh with a resolution of 1mm. Due to the symmetry of this detection model, only one-fourth of the scanning grid results are needed in simulation.

The simulation of experimental set-up including light illumination and signal measurements is executed using a Monte Carlo program adapted from Guo et al. [23]. Modifications have been made to the program code to consider the presence of tumors. The Monte Carlo simulation mimics photon propagation by calculating the random walks of a large number of photon bundles. Each emitted photon bundle begins from its initial position and time before making its way into the participating medium by a certain path length determined from statistical distribution and given by the equation:

$$l = -\frac{1}{\mu_e}\ln(\Re) \tag{1}$$

where $\mu_e$ represents the extinction coefficient of the medium and $\Re$ the random number generated by the computer. The photon bundle will experience scattering, absorption, or reflection at tissue-air interfaces before being detected. Fresnel reflection [17] at the tissue-air boundary is considered because there is a significant refractive index mismatch between tissue and air. Total internal reflection occurs when the incoming angle is not less than the critical angle as determined by Snell's law. The energy attenuation due to absorption is calculated using the Beer-Lambert law:

$$I_{i+1} = I_i e^{-\mu_a l} \tag{2}$$

where $I_i$ and $I_{i+1}$ are photon bundle energy before and after each scattering event, respectively, $l$ is the path length calculated from equation (1), and $\mu_a$ is the absorption coefficient of the medium along each scattering path length and varies depending on whether it is inside healthy tissue or inside the tumor. In the event where the photon bundle's path traverses both the normal tissue and tumor regions, the overall energy attenuation is calculated from two successive attenuations in the tissue and tumor regions, respectively. The first attenuation will be based on the distance to the tissue-tumor interface with the current extinction coefficient, while the second attenuation is based on the remaining path length with the extinction coefficient corresponding to the medium that the photon bundle is traveling towards. The remaining path length $l_2$ is calculated based on the conservation of optical depth and is given by:

$$l_2 = \frac{\mu_{e1}(l_0 - l_1)}{\mu_{e2}} \tag{3}$$

where $l_0$ corresponds to the path length of the originally intended travel distance calculated from Eq. (1), and $l_1$ corresponds to the distance to the tissue-tumor interface from the starting point. The constants $\mu_{e1}$ and $\mu_{e2}$ refer to the extinction coefficients of the medium before and after the tissue-tumor interface. In our simulation, we used a total of $10^8$ photon bundles on each node of the scanning grid.

A single detecting point calculation takes about 2 hours on a DELL PC equipped with a 1.7GHz Pentium IV processor and 256MB memory. The simulation on the top surface of the tissue phantom requires 361 runs for detection model with a 19 x 19 scanning grid. The calculation task is too heavy for a single PC. Accordingly, the final calculations were conducted in a 64-CPU workstation cluster. It must be pointed out that the above-mentioned computational effort was for simulating an experimental setup to obtain a "simulated" measurement. It is not used for image processing and reconstruction. If a practical experiment is set up, real measurement can be completed in minutes, and the previous simulation process is not necessary.

Due to the high-scattering and low-absorption of NIR light in tissues, detected signal pulses at the boundary will be broadened considerably. At the decaying part of the signal, there exists an asymptotic log-slope region that is sensitive to the distribution of absorption coefficients inside the tissue phantom [20]. From our experience, the log-slope is best chosen in the time range of 300-700ps. Prior to 300 ps the logarithmic signal is non-linear, while after 700 ps the signal strength is weak and the signal is strongly affected by a large zone beyond the optical axis.

In order to form a 2-D mapping of log-slope difference to detect the tumor's projection onto the tissue surface, we first

evaluate the log-slope distribution before the administration of absorbing contrast agent. This evaluation is followed by evaluation of the log-slope distribution after absorption enhancement. Then, a 2-D mapping of log-slope difference between these two log-slope distributions can be constructed. Due to the affinity of absorbing contrast agent for cancerous regions, the log-slope difference is significantly larger in the tumor region than in other regions. This mechanism is illustrated in Fig. 2 which shows log-slope profiles versus *x*-position plotted along $y$ = 10mm for the simulation model in three different cases: before absorption enhancement, after absorption enhancement, and the net difference between the previous two profiles.

For the simulation model, we obtained one set of log-slope distributions corresponding to the cases before and after the addition of contrast agent, respectively. By proceeding with the log-slope subtraction process, a log-slope difference mapping was constructed. In the cancerous region, the difference is large. A final filtering process was applied to highlight the image contrast and to suppress unwanted noise. Values below a pre-assigned cut-off filter level were removed. The computation in image processing and mapping construction took between two to three minutes on a 1.7 GHz Pentium IV PC.

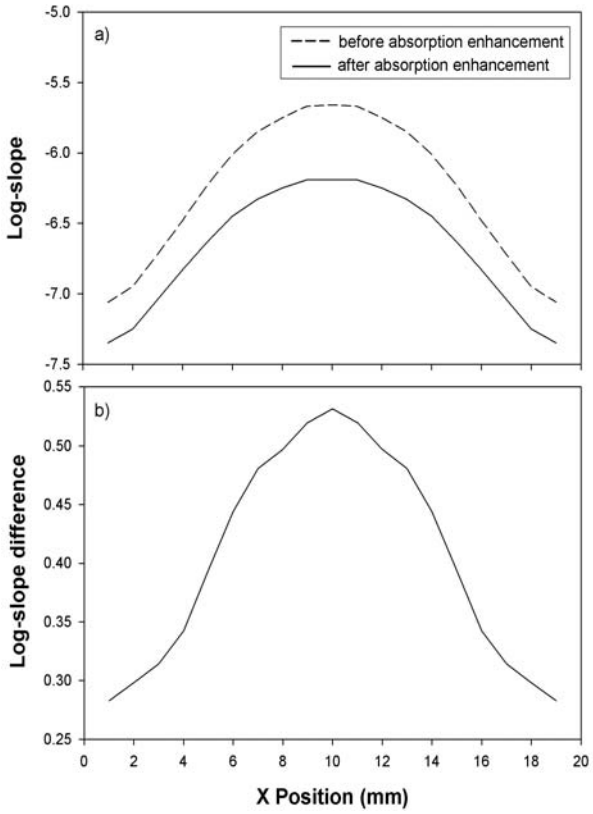


Figure 2 – (a) Plots of log-slope versus *x*-position along $y$ = 10mm; and (b) profile of log-slope difference.

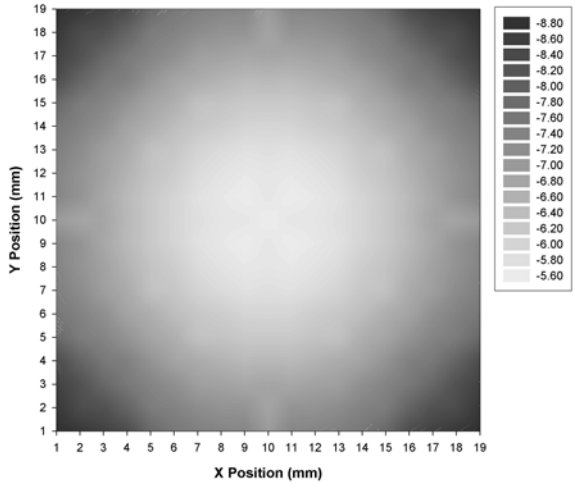


Figure 3 – Log-slope mapping results before administration of contrast agent.

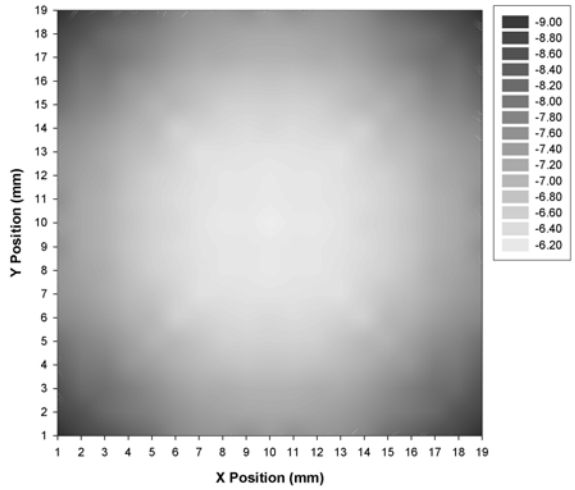


Figure 4 – Log-slope mapping results after administration of absorption contrast agent.

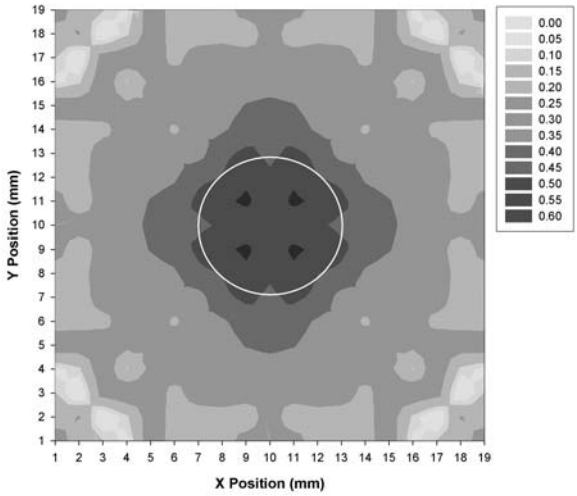


Figure 5 – Mapping of log-slope difference between log-slope distributions before and after absorption enhancement.

## RESULTS AND DISCUSSION

The complete log-slope distributions of detection model are presented in Figs. 3 and 4. Figure 3 shows the log-slope mapping on a surface of the cuboidal tissue phantom before administration of absorbing contrast agent. The log-slope values range from –5.60 to –8.80. The presence of tumor is not immediately identifiable due to the strong edge effect associated with the relatively small geometry in this detection model. Figure 4 shows the result after absorption enhancement. The log-slope values range from –6.20 to –9.20. The absolute values of the log-slopes increase. This indicates that the decay of the log-slope signal has become steeper since more energy is absorbed by the absorption-enhanced tumor.

Figure 5 was obtained by subtracting the log-slopes in Fig. 4 from the corresponding values in Fig. 3. The initial subtraction created log-slope difference values that fell between 0.05 and 0.53 for the whole 2-D distribution. A larger difference value indicates stronger absorption augmentation in the cancerous region. In this simulation result, the majority of the higher values (above 0.42) were concentrated on the region where the tumor is located. The presence of tumor at the center in Fig. 5 is clearly visible. Figures 6-8 show images of the tumor projection on the detection surface after applying various filters to the image in Fig. 5. The cut-off filter value is 60% of the peak log-slope difference value in Fig. 6, 70% in Fig. 7, and 80% in Fig. 8, respectively. As the cut-off filter value increased, the effective imaging area representing the tumor projection decreased accordingly and the image quality became better. A 80% cut-off filter level was found to produce images clear enough for visualizing the tumor projection (indicated by the white circle in the figures). A more general and effective cut-off filter value can be established when more cases are simulated and analyzed. Although the filtered log-slope difference image corresponds well to the shape and location of the actual tumor, the image boundary does not resemble a perfect circle. The main reason is due to the limited resolution of the scanning grid defined in the simulation model. Further increase in resolution should result in a better image quality.

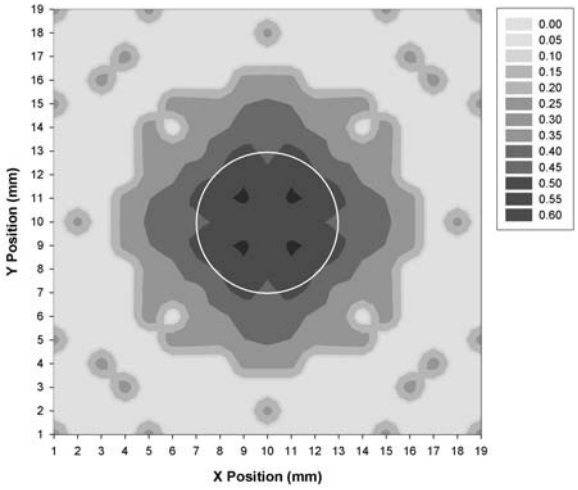


Figure 6 – Mapping of log-slope difference with 60% cut-off filter.

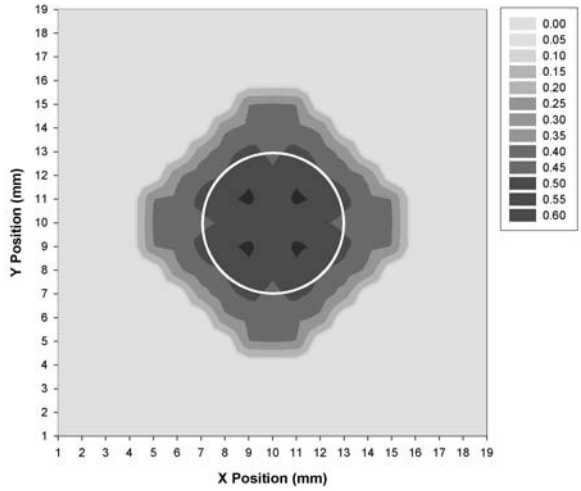


Figure 7 – Mapping of log-slope difference with 70% cut-off filter.

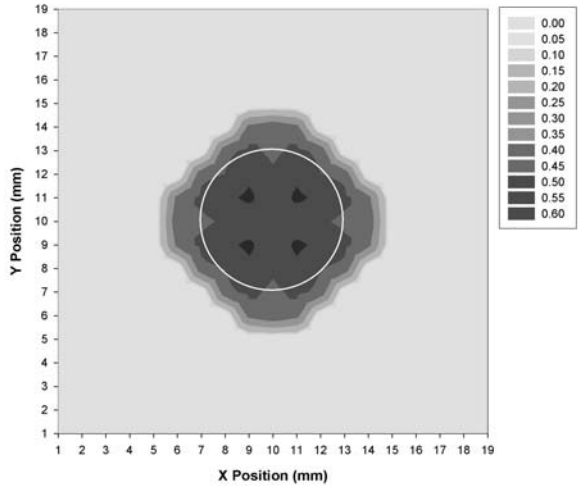


Figure 8 – Mapping of log-slope difference with 80% cut-off filter.

## CONCLUSION

This study evaluated a novel tumor detection method based on NIR log-slope difference mapping of transient radiation signals. The concept of this approach as a quick yet accurate preliminary diagnostic tool for early cancer detection was demonstrated through simulations. The temporal log-slope difference between tissues before and after absorption enhancement was shown to be very large for those detection points directly above the embedded tumor. The results in the two example detection models accurately showed the shape and location of the embedded tumors. The proposed temporal log-slope difference mapping method is capable of forming 2-D tumor projection for the detection of cancerous tumors. The images were directly constructed. The image processing and construction took only a couple of minutes in a PC. The present imaging method does not require any inverse image reconstruction. These features will greatly enhance the clinical utility of the present method.

We have shown this projection imaging capability for only one surface of the tissue. Clearly this method can produce temporal log-slope difference mappings for multiple scanning surfaces throughout the entire tissue. The projection of the tumor onto multiple surfaces would produce log-slope difference maps that can be combined to produce a 3-D image. This as well as feasibility demonstration in more realistic situations and experimental studies will be the focus of our future reports

## ACKNOWLEDGEMENTS

Z. Guo acknowledges the partial support of this research from the New Jersey Space Grant Consortium, the Charles and Johanna Busch Memorial Fund, and the NSF grant (CTS-0318001).

## REFERENCES

[1] B. Tromberg, A. Yodh, E. Sevick-Muraca and D. Pine, 1997, "*Diffusing photons in turbid media: introduction to the feature*," Appl. Optics, vol. 36, pp. 9-231.

[2] M.J. Holboke, B. J. Tromberg, X. Li, N. Shah, J. Fishkin, D. Kidney, J. Butler, B. Chance, A. G. Yodh, 2000, "*Three-dimensional diffuse optical mammography with ultrasound localization in a human subject*", J. Biomedical Optics, vol. 5, pp. 237-247.

[3] Roy R, Godavarty A, Sevick-Muraca EM, 2003, "*Fluorescence-enhanced optical tomography using referenced measurements of heterogeneous media*", IEEE Transactions on Medical Imaging, vol. 22, pp. 824-836.

[4] J. C. Hebden, H. Veenstra, H. Dehghani, E. M. C. Hillman, M. Schweiger, S. R. Arridge, and D. T. Delpy, 2001, "*Three dimensional time-resolved optical tomography of a conical breast phantom*," Applied Optics, vol. 40, pp. 3278-3287.

[5] J. P. Culver, R. Choe, M. J. Holboke, L. Zubkov, T. Durduran, A. Slemp, V. Ntziachristos, B. Chance, and A. G. Yodh, 2003, "*Three-dimensional diffuse optical tomography in the parallel plane transmission geometry: Evaluation of a hybrid frequency domain/continuous wave clinical system for breast imaging*," Medical Physics, vol. 30, no. 2, pp. 235-247.

[6] B. W. Pogue, S. Geimer, T. O. McBride, S. D. Jiang, U. L. Osterberg, and K. D. Paulsen, 2001, "*Three-dimensional simulation of near-infrared diffusion in tissue: boundary condition and geometry analysis for finite-element image reconstruction*," Applied Optics, vol. 40, pp. 588-600.

[7] H. Jiang, Y. Xu, N. Iftimia, J. Eggert, K. Klove, L. Baron, L. Fajardo, M. A. Bartlett, H. Jiang, 2001, "*Effect of refractive index on the measurement of optical properties in turbid media*," J. Opt. Society America, vol. 40, no. 10, pp. 1735-1741.

[8] J. Wu, L. Perelman, R. R. Dasari, and M. S., Feld, 1997, "*Fluorescence tomographic imaging in turbid media using early-arriving photons and Laplace tranforms*", PNAS, vol. 94, pp. 8783-8788.

[9] D. A. Benaron, S. R. Hintz, A. Villringer, D. Boas, A. Kleinschmidt, J. Frahm, C. Hirth, H. Obrig, J. C. van Houten, E. L. Kermit, W. F. Cheong and D. K. Stevenson, 2000, "*Noninvasive functional imaging of human brain using light*," J. Cereb. Blood Flow Metab., vol. 20, pp. 469-477.

[10] B. J. Tromberg, N. Shah, R. Lanning, A. Cerussi, J. Espinoza, T.Pham, L. Svaasand, J. Butler, 2000, "*Non-invasive in vivo characterization of breast tumor using photon migration spectroscopy*," Neoplasia, vol. 2, pp. 1-15.

[11] D. A. Boas, G. Strangman, J. P. Culver, R. D. Hoge, G. Jasdzewski, R. A. Poldrack, B. R. Rosen and J. B. Mandeville, 2003, "*Can the cerebral metabolic rate of oxygen be estimated with nearinfrared spectroscopy?*," Phys. Med. Biol., vol. 48, 2405-2418.

[12] V. Ntziachristos, A. G. Yodh, M. Schnall, B. Chance, "*Concurrent MRI and diffuse optical tomography of breast after indocyanine green enhancement*," PNAS, vol. 97, no. 6 pp. 2767-2772 (2000).

[13] E. Betzig, 1995, "*Proposed method for molecular optical imaging*," Optics Letter, vol. 20, no. 3, pp. 237-239.

[14] R. Weissleder, C. H. Tung, U. Mahmood, A. Bogdanov Jr., 1999, "*In vivo imaging of tumor with protease-activated near-infrared fluorescent probes*," Nature Biotech., vol. 17, pp. 375-378.

[15] Z. Guo, S. K. Wan, K.-H. Kim, and C. Kosaruja, 2003, "*Comparing Diffusion Approximation with Radiation Transfer Analysis for Light Transport in Tissues*", Optical Review, vol. 10, no. 5, pp. 415-421.

[16] Z. Guo and Kumar, 2001, "*Discrete Ordinates Solution of Short Pulse Laser Transport in Two-Dimensional Turbid Media*," Applied Optics, vol. 40, no.19, pp. 3156-3163.

[17] Z. Guo, and K. H. Kim, 2003, "*Ultrafast Laser Radiation Transfer in Heterogeneous Tissues Using Discrete Ordinates Method*," Applied Optics, vol. 42, no. 16, pp. 2897-2905.

[18] S. K. Wan, Z. Guo, S. Kumar, J. Aber and B. A. Garetz, 2004, "*Noninvasive detection of inhomogeneity in turbid media time-resolved log-slop analysis*," J. Quantitative Spectroscopy and Radiative Transfer, vol. 84, no. 4, pp. 493-500.

[19] F. Liu, K. M. Yoo and R. R. Alfano, 1993, "*Ultrafast laser-pulse transmission and imaging through biological tissues*," Applied Optics, vol. 32, no. 4, pp. 554-558.

[20] M. Q. Brewster, Y. Yamada, 1995, "*Optical properties thick, turbid media from picosecond time resolved light scattering measurements*," Int. J. Heat Mass Transfer, vol. 38, pp. 2569-2581.

[21] G. Zaccanti, P. Bruscaglioni, A. Ismaelli, L. Carraresi, M. Gurioli and Q. Wei, 1992, "*Transmission of a pulse thin light beam through thick turbid media: experimental results*," J. Opt. Society America, vol. 31, no. 12, pp. 2141-2147.

[22] Z. Guo, S. Kumar, K. C. San, 2000, "*Multidimensional Monte Carlo simulation of short-pulse laser transport in scattering media*," J. Thermophysics Heat Transfer, vol. 14, no. 4, pp. 504-511.

[23] Z. Guo, J. Aber, B. Garetz and S. Kumar, 2002, "*Monte Carlo simulation and experiments of pulsed radiative transfer*," Journal of Quantitative Spectroscopy and Radiative Transfer, vol. 73, pp. 159 – 168.

[24] S. Kumar and K. Mitra, 1999, "*Microscale aspects of thermal radiation transport and laser applications*," Adv. Heat Transfer, vol. 33, pp. 187-294.

[25] M. Sakami, K. Mitra, and P. Hsu. 2002, "*Analysis of light-pulse transport through two-dimensional scattering-absorbing*

*media*," Journal of Quantitative Spectroscopy and Radiative Transfer, vol. 73, pp. 169–179.
[26] B.T. Wong and M.P. Mengüç, 2002, "*Comparison of Monte Carlo techniques to predict the propagation of a collimated beam in participating media*," Numerical Heat Transfer, Vol. 42, pp. 119-140, 2002.
[27] B. Chance, S. Nioka, J. Kent, K. McCully, M. Fountain, R. Greenfeld and G. Holtom, 1988, "Time-resolved spectroscopy of hemoglobin and myoglobin in resting and ischemic muscle", Anal. Biochem., vol. 174, pp. 698-707.
[28] M.S. Patterson, B. Chance and B.C. Wilson, 1989, "Time-resolved reflectance and transmittance for the noninvasive measurement of tissue optical properties," Applied Optics, vol. 28, pp. 2331-2336.